Supporting Information

Novel cerium and praseodymium doped phosphate tungsten bronzes: Synthesis, characterization, photoluminescent properties and behavior in Briggs-Rauscher reaction

Tijana Maksimović[a], Pavle Tančić[b], Jelena Maksimović[c], Dimitrije Mara[d,e], Marija Ilić[f], Rik Van Deun[g], Ljubinka Joksović[a], Maja Pagnacco[b*]

a. Department of Chemistry, Faculty of Science, University of Kragujevac, Radoja Domanovića 12, 34000 Kragujevac, Serbia
b. Institute of Chemistry, Technology and Metallurgy, University of Belgrade, Njegoševa 12, 11000 Belgrade, Serbia
c. Faculty of Physical Chemistry, University of Belgrade, Studentski trg 12-16, 11001 Belgrade, Serbia
d. Molecular Imaging and Photonics, Department of Chemistry, KU Leuven, Celestijnenlaan 200 D, box 2425, B-3001, Leuven, Belgium
e. Institute of General and Physical Chemistry, Studentski trg 12/V, 11158, P.O. box 45, Belgrade, Serbia
f. Faculty of Mining and Geology, University of Belgrade, Djušina 7, 11120 Belgrade, Serbia
g. L^3 – Luminescnet Lanthanide Lab, Department of Chemistry, Ghent Univeristy, Krijgslaan 281 – S3, B-9000, Ghent, Belgium

*coresponding author: maja.pagnacco@nanosys.ihtm.bg.ac.rs or maja.milenkovic@ymail.com

Structural and thermal analysis of Ce-PWA, Pr-PWA, Ce-PWB, and Pr-PWB

In Fig. S1 is shown the FTIR spectrum of 6-PWA, at room temperature. In the spectrum of 6-PWA are characteristic bands of molecule H_2O, PO_4 tetrahedral, and WO_6 octahedral. The band at 3404 cm^{-1} corresponds to ν (H_2O) vibration, while the band at 1636 cm^{-1} corresponds to δ (H_2O) vibration. The IR characteristic bands of the Keggin's anion structure are: the band at 1080 cm^{-1} pertains to ν_3 (PO_4) vibration, the band at 983 cm^{-1} corresponds to vibration of ν_1 (PO_4) tetrahedron, the band at 889 cm^{-1} corresponds to ν (W = O) vibration, the band at 802 cm^{-1} confirms the vibration ν (O-W-O), the band at 595 cm^{-1} can be assigned to the vibration ν_4 (PO_4) of the tetrahedron and the band at 525 cm^{-1} corresponds to the ν_2 (PO_4) vibration.

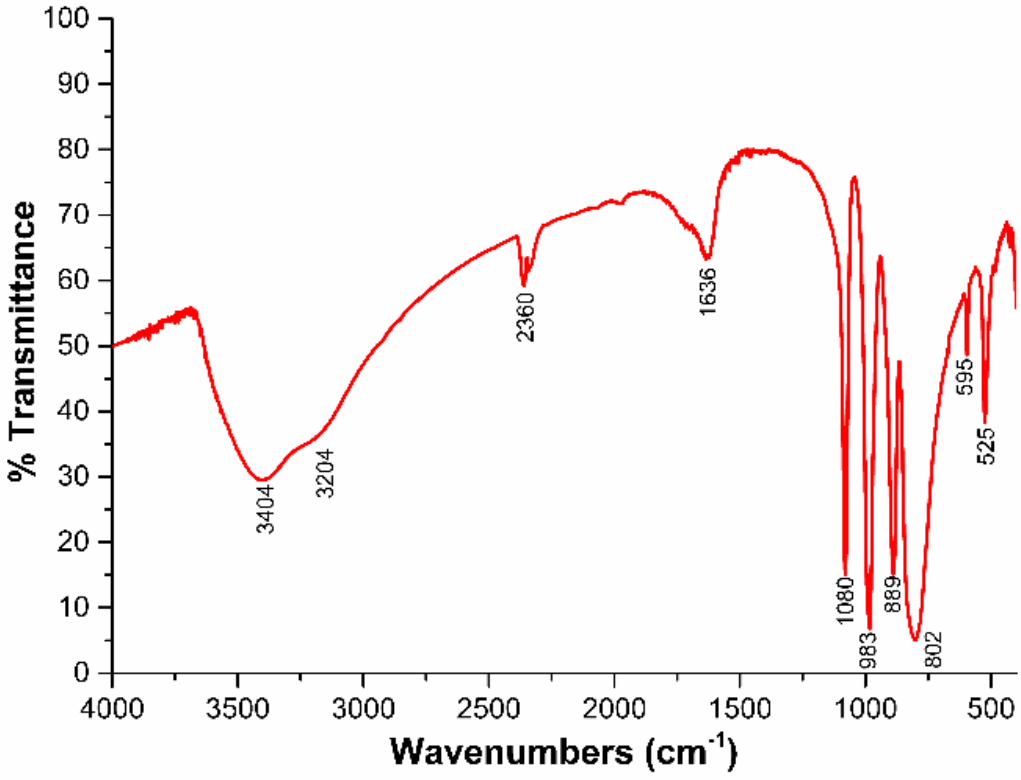

Fig. S1 FTIR spectrum of 6-PWA

The observed XRPD patterns of Ce and Pr doped phosphate tungsten acids (Ce-PWA and Pr-PWA, respectively) are shown in Fig. 3 and in Table S1. It is obvious that the determined data for studied acids more or less differs among each other, and also with the data for cubic 6-PWA (calcined at the ~60-170 °C region [30]) and for Ca-PWA (calcined at 170 °C [41]). This fact could primarily indicate that these two studied compounds most probably were not dehydrated enough and that contain more than 6 molecules of water, i.e., that 6-PWA structure was not completely achieved at 80 °C.

Table S1 Observed inter-planar spacings (d_{obs}, in Å) and intensities (I_{obs}, in %) of Ce-PWA and Pr-PWA, in comparison with 6-PWA and Ca-PWA

6-PWA[1]			**Ca-PWA**[2]		**Ce-PWA**		**Pr-PWA**	
h k l	**d_{obs}**	**I_{obs}**	**d_{obs}**	**I_{obs}**	**d_{obs}**	**I_{obs}**	**d_{obs}**	**I_{obs}**
1 1 0	8.580	66	8.55	37			8.612(6)	32
1 1 1	7.008	2			6.900(6)	7	6.936(3)	7
2 0 0	6.073	16	6.05	11	5.81(9)	1	6.080(3)	9
2 1 1	4.961	15	4.93	88	4.943(2)	15	4.973(7)	33
					4.825(2)	14		
2 2 0	4.297	36	4.28	100	4.408(2)	65	4.437(2)	74
					4.339(2)	52	4.362(2)	65
							4.304(4)	20
2 2 1	4.052	1			4.022(9)	5	4.038(7)	5
3 1 0	3.843	24	3.84	19			3.850(3)	16
			3.60	29	3.6441(8)	82	3.658(2)	100
2 2 2	3.508	100	3.50	69	3.496(4)	7	3.509(3)	62
					3.424(4)	5		
3 2 1	3.248	4			3.262(1)	40	3.2721(6)	35
					3.2225(8)	22	3.232(2)	14
			3.10	37	3.125(3)	8	3.139(3)	10
4 0 0	3.039	29	3.04	21	3.087(1)	28	3.0986(9)	29
							3.041(2)	18
							2.990(4)	7
					2.911(2)	43	2.921(2)	37
3 3 0	2.864	13	2.87	25	2.8309(6)	100	2.8480(6)	59
					2.8185(4)	41		
4 2 0	2.717	7			2.700(3)	10	2.710(1)	12
					2.6328(8)	10	2.637(2)	11
3 3 2	2.590	51	2.59	40			2.591(1)	29
					2.526(1)	8	2.534(2)	9
			2.44	19	2.4734(3)	11	2.481(2)	10
					2.4347(7)	7	2.4422(3)	9
					2.4189(5)	23	2.4264(5)	18
5 1 0	2.383	23	2.38	54	2.3836(7)	35	2.3894(4)	51
5 1 1	2.338	1			2.3530(7)	5	2.3583(7)	4
					2.2673(3)	9	2.274(2)	8
5 2 1	2.218	5	2.22	5	2.2401(3)	32	2.2460(2)	24
					2.212(5)	4	2.220(1)	8
4 4 0	2.148	4			2.152(1)	15	2.1570(6)	16
					2.122(1)	16	2.1290(3)	16
5 3 0	2.085	2			2.0743(9)	13	2.078(1)	13
6 0 0	2.025	6					2.026(4)	4
6 1 1	1.971	13	1.97	59	1.971(1)	8	1.9744(5)	18
6 2 0	1.921	4					1.9383(9)	4
							1.9195(3)	4
							1.9092(3)	5
5 4 0	1.898	2			1.891(1)	5	1.8963(5)	9
5 4 1	1.875	7					1.879(2)	4
6 2 2	1.832	2			1.832(5)	10	1.8355(5)	9
					1.8146(3)	37	1.8170(4)	36
4 4 4	1.753	1			1.774(1)	6		
7 1 0	1.719	20	1.72	25	1.732(1)	7	1.7349(8)	6

							1.7215(8)	15
					1.707(1)	6		
6 4 0	1.685	2			1.6924(4)	15	1.6956(5)	8
7 2 1	1.654	2			1.639(1)	9	1.639(2)	6
6 4 2	1.623	1			1.6123(6)	6	1.6140(9)	7
					1.6034(4)	17	1.6059(5)	15
7 3 0	1.595	1			1.5803(7)	9	1.5823(4)	7
6 5 1	1.543	18	1.54	35	1.5642(6)	14	1.5656(4)	12
					1.5361(5)	5	1.5456(2)	14
8 1 1	1.496	8	1.50	13	1.5043(8)	10	1.5055(5)	5
8 2 0	1.474	2			1.484(1)	4		
6 5 3	1.452	1			1.4678(5)	9	1.4681(8)	5
6 6 0	1.433	5			1.4493(6)	9	1.4510(3)	7
					1.441(1)	6	1.4356(8)	3
7 5 0	1.412	1						
7 5 2	1.376	2			1.3594(7)	2	1.357(1)	2

[1)] Ref [30], [2)] Ref [41]

Contrariwise, XRPD patterns of Ce and Pr doped phosphate tungsten bronzes (Ce-PWB and Pr-PWB, respectively; Fig. 4 and Table S2 are very similar and highly comparable between each other. It can be also emphasized here that peaks with the highest intensities for Ce-PWB and Pr-PWB (i.e., at about 23-24^o, 33-34^o, and 53.5-56^o angle 2θ ranges) are quite similar to Ca-PWB [41]. These peaks are without expressively visible doublets which are characteristic for PWB [30], but broadened and with more or fewer shoulders present, which could indicate two (or more) diffraction maximums. Therefore, it is obvious that the observed data for these studied bronzes are analogical to those obtained for PWB crystallized as monoclinic at temperature conditions of 750 °C {ICDD-PDF (International Centre for Diffraction Data-Powder Diffraction File): 50-0660 [30]}, and for Ca-PWB crystallized at temperature conditions of 650 °C [41], as well. This fact primarily indicates that these four phases are iso-structural between each other.

Table S2 Observed inter-planar spacings (d_{obs}, in Å) and intensities (I_{obs}, in %) of Ce-PWB and Pr-PWB, in comparison with PWB, Ca-PWB, and Li-PWB

PWB[1]			**Ce-PWB**		**Pr-PWB**		**Ca-PWB**[2]		**Li-PWB**	
h k l	$\mathbf{d_{obs}}$	$\mathbf{I_{obs}}$	$\mathbf{d_{obs}}$	$\mathbf{I_{obs}}$	$\mathbf{d_{obs}}$	$\mathbf{I_{obs}}$	$\mathbf{d_{obs}}$	$\mathbf{I_{obs}}$	$\mathbf{d_{obs}}$	$\mathbf{I_{obs}}$
0 0 2	3.840	41					3.810(2)	33	3.840	100
0 2 0	3.749	100	3.743(2)	100	3.749(2)	100	3.726(2)	100	3.757	81
2 0 0									3.653	85
-1 2 0	3.337	1							3.344	15
-1 1 2	3.108	6	3.099(6)	10						
1 1 2	3.083	5			3.092(2)	7	3.091(6)	13	3.099	15
0 2 2									2.687	29
-2 0 2	2.677	40	2.663(1)	68	2.6632(8)	62	2.6567(9)	64		
2 0 2	2.637	26								
-2 2 0									2.620	42
1 2 2									2.523	5
2 2 2									2.166	10
-2 2 2	2.173	14	2.173(2)	17	2.178(1)	16	2.1687(6)	12		
-3 2 0									2.045	2
2 1 3	2.006	2			2.001(4)	2	1.992(4)	3		
1 3 2									2.018	2
3 1 2									1.987	5
0 0 4	1.922	3							1.921	7
0 4 0									1.880	8
-1 0 4	1.866	11	1.877(4)	9	1.869(2)	9				
0 1 4	1.861	10					1.8583(7)	18		
0 4 1									1.825	18
3 2 2									1.806	10
-1 1 4	1.810	4			1.803(3)	5	1.793(2)	12		
0 2 4	1.712	6							1.710	9
-3 3 1	1.708	6								
0 4 2									1.691	7
-2 4 0									1.672	9

-2 1 4	1.668	15	1.678(1)	23	1.6782(8)	18	1.6671(3)	40		
1 4 2									1.646	16
2 3 3	1.603	1								
-2 2 4	1.555	3								
2 4 2	1.530	9	1.534(1)	14	1.5360(8)	11	1.5279(9)	18	1.534	5
4 2 2									1.512	5
4 0 3									1.490	8
-1 4 3	1.487	3			1.484(2)	4	1.484(3)	7		
3 4 2									1.389	2
			1.330(3)	4	1.332(2)	3	1.325(2)	6		
			1.253(2)	7	1.253(1)	5	1.249(1)	14		

1) Ref [30], [2)] Ref [41]

Table S3 Calculated inter-planar spacings (d_{calc}, in Å) of Ce-PWB, Pr-PWB, Ca-PWB, and Li-PWB in comparison with PWB

	PWB[1]	**Ce-PWB**	**Pr-PWB**	**Ca-PWB**	**Li-PWB**
h k l	**d_{calc}**	**d_{calc}**	**d_{calc}**	**d_{calc}**	**d_{calc}**
0 0 2	3.843			3.823	3.841
0 2 0	3.758	3.759	3.764		3.761
2 0 0				3.721	3.655
-1 2 0	3.344				3.344
-1 1 2	3.114	3.096			
1 1 2	3.086		3.083	3.090	3.101
0 2 2					2.687
-2 0 2	2.669	2.667	2.672		
2 0 2	2.633			2.658	
-2 2 0					2.621
1 2 2					2.524
-2 2 2	2.176	2.175	2.179		
2 2 2				2.168	2.167
-3 2 0					2.045
1 3 2					2.019
2 1 3	2.010		2.007		
3 2 1				1.994	
3 1 2					1.987
0 0 4	1.921				1.921
0 4 0		1.880			1.880
4 0 0				1.861	
-1 0 4	1.865		1.864		
0 1 4	1.862				
0 4 1					1.826
3 2 2					1.807
-1 1 4	1.810		1.810		
1 1 4				1.795	
0 2 4	1.711				1.710
-2 0 4	1.711				
-3 3 1	1.708				
2 0 4	1.692				
0 4 2					1.689
-2 4 0		1.678	1.674		1.672
4 0 2				1.669	
-2 1 4	1.668				
1 4 2					1.646
2 3 3	1.603				
-2 2 4	1.557				
0 0 5			1.536	1.529	
2 4 2	1.530	1.535			1.534
4 2 2					1.512

1 3 4				1.486	
4 0 3					1.489
-1 4 3	1.486		1.488		
3 4 2					1.389
-2 2 5			1.332		
4 0 4		1.331			
-2 2 5				1.326	
-1 0 6		1.254			
-4 4 2				1.250	
0 6 0			1.254		

[1)] Ref [30]

Considering the previous discussion, the unit cell dimensions of Ce-PWB, Pr-PWB, Ca-PWB, and Li-PWB were calculated in the present paper in monoclinic symmetry starting from the initial data for PWB (ICDD-PDF: 50-0660 [30]), and presented at Table S3 and Table 1. The obtained results indicate that these values are, as expected, more or less varying between the different bronzes. We believe that one of the primary reasons for such behavior could be various ionic radiuses of included different dopants. Accordingly, there were chosen following values for coordination number VIII [51], of: 1.143Å, 1.126Å, 1.12Å, and 0.92Å for Ce^{3+}, Pr^{3+}, Ca^{2+}, and Li^{+}, respectively. Variations of such ionic radiuses by unit cell dimensions are studied for different bronzes and presented in Figure S2. For every variation, there were further calculated linear and polynomial coefficients of the regression (R^2; hereinafter coefficients-C), which was previously shown to be a very useful accessory tool for different correlation parameters [52].

From Figure S2, it can be seen that polynomial variations are something better than the linear. Also, it is obvious that various dopants in the studied bronzes more or less affecting to their structures. Namely, a_0 axis, angle β_0 and volume V_0 increase, whereas b_0 and c_0 axes decrease with the increase of dopants ionic radiuses. More specifically, relatively good coefficients (C1) can be associated with the a_0, c_0, β_0 and V_0 parameters (0.510; 0.556; 0.662; and 0.702; respectively), whereas axis b_0 shows very poor correlation (0.182). Deviations from better correlation coefficients from these could be found by the fact that Ce^{3+} and Pr^{3+} belong to the same REEs group, whereas Ca^{2+} and Li^{+} belong to the other chemical groups and have different electro-negativity.

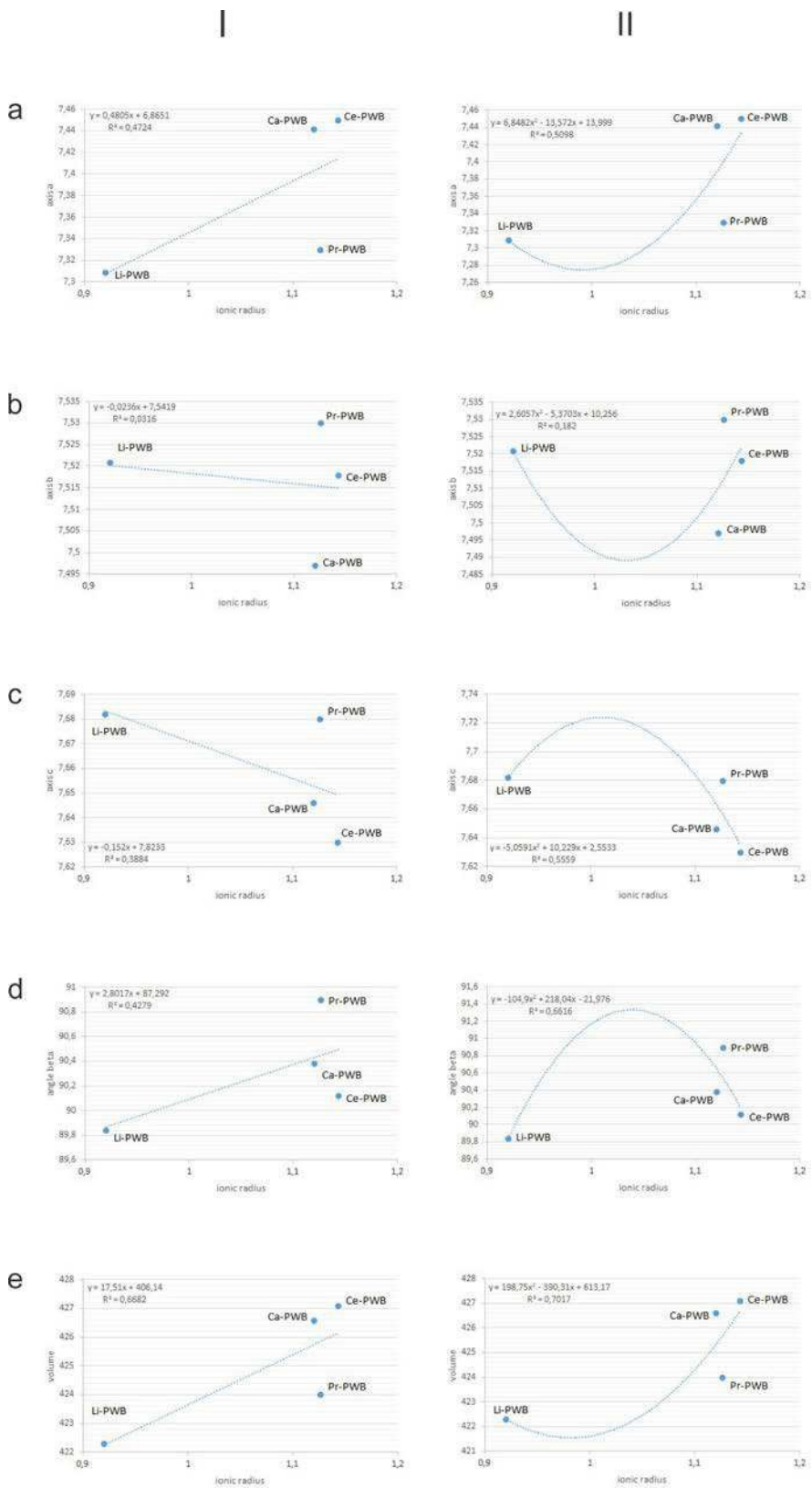

Figure S2 Linear (column I, left) and polynomial (column II, right; C1) variations of ionic radiuses (in Å) for Ce-PWB, Pr-PWB, Ca-PWB and Li-PWB bronzes by: a) axis a_0 (in Å); b) axis b_0 (in Å); c) axis c_0 (in Å); d) angle β_0 (in ^{o}); and e) volume V_0 (in $Å^3$)

On the other hand, second option that could be considered is that praseodymium is characterized as Pr^{4+} (0.96Å for coordination number VIII [51]). In that case, excellent coefficients (C2; Figure S3) were obtained for the a_0, c_0, β_0 and V_0

parameters (0.998; 0.992; 0.910; and 0.992; respectively). Similarly, much better values were also obtained for the b_0 axis (0.416).

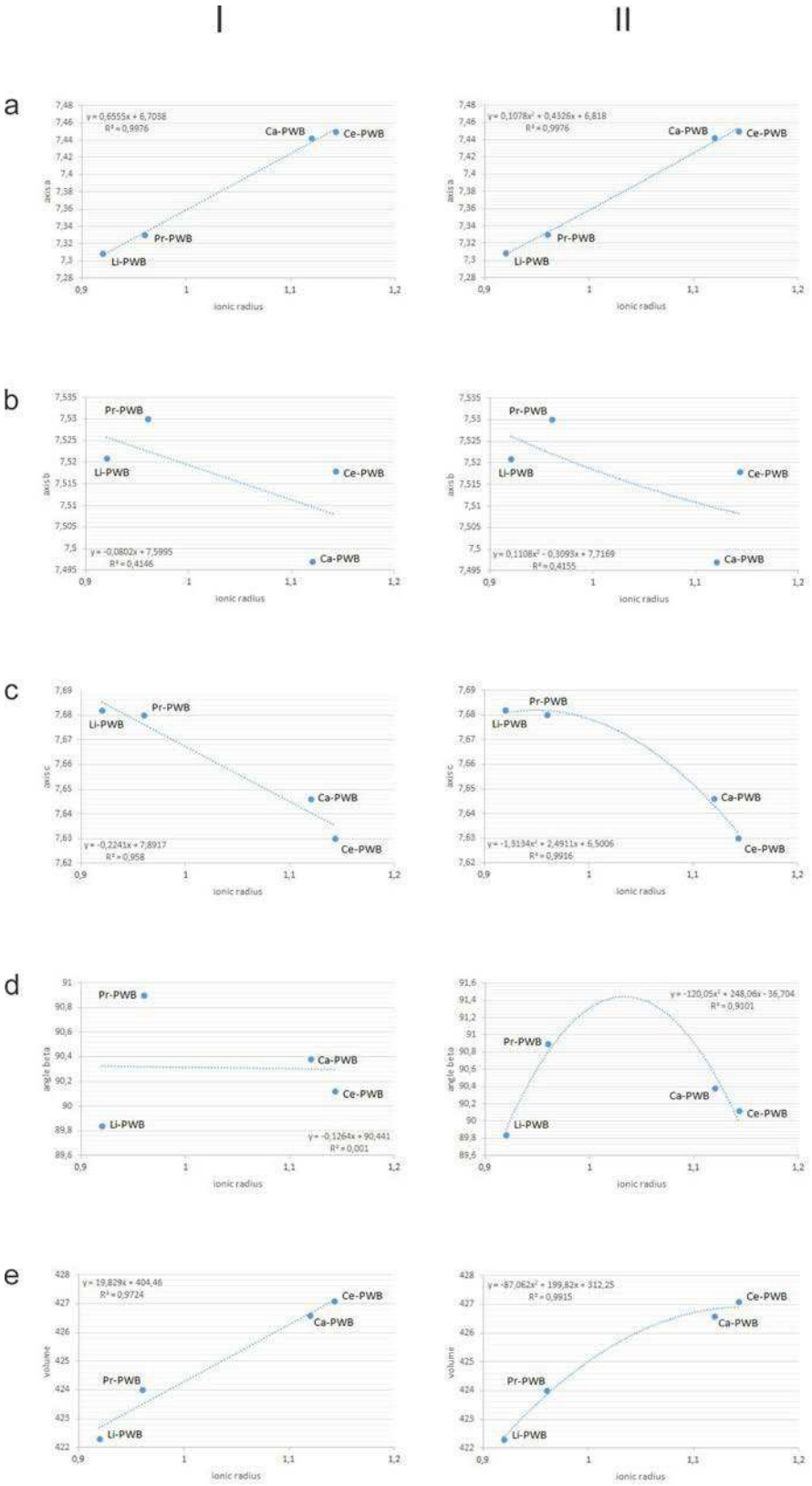

Figure S3 Linear (column I, left) and polynomial (column II, right; C2) variations of ionic radiuses (in Å) for Ce-PWB, Pr-PWB, Ca-PWB and Li-PWB bronzes by: a) axis a_0 (in Å); b) axis b_0 (in Å); c) axis c_0 (in Å); d) angle β_0 (in ^{o}); and e) volume V_0 (in $Å^3$)

Furthermore, we considered another two more possible options. Namely, third option that was taken into account is that Ce^{3+}, Pr^{3+}, Ca^{2+}, and Li^{+} are with the coordination number VI [51], having ionic radiuses of: 1.01Å, 0.99Å, 1.00Å, and 0.76Å for Ce^{3+}, Pr^{3+}, Ca^{2+}, and Li^{+}, respectively. The resulting coefficients (C3; Figure S4) are also excellent and significantly better than those for coordination number VIII (C1), having following values for the a_0, c_0, β_0 and V_0 parameters of: 0.879; 0.966; 0.976; and 0.946; respectively. On the contrary, axis b_0 shows also very poor correlation (0.155).

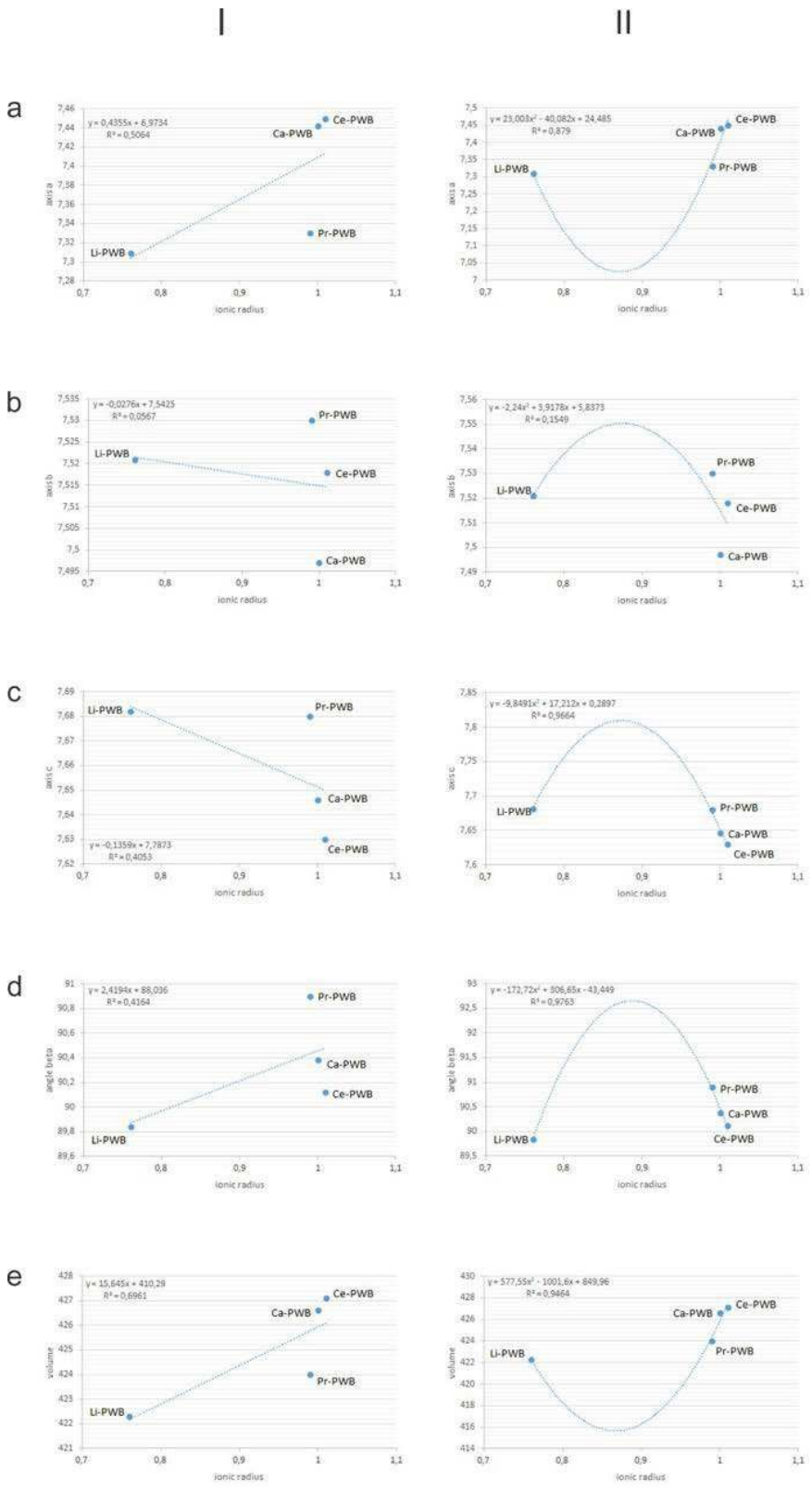

Figure S4 Linear (column I, left) and polynomial (column II, right; C3) variations of ionic radiuses (in Å) for Ce-PWB, Pr-PWB, Ca-PWB and Li-PWB bronzes by: a) axis a_0 (in Å); b) axis b_0 (in Å); c) axis c_0 (in Å); d) angle β_0 (in ^{o}); and e) volume V_0 (in $Å^3$)

At last, fourth option that was considered is that praseodymium is also characterized as Pr^{4+} (0.85Å for coordination number VI [51]). The resulting coefficients (C4; Figure S5) are the best among all of the four options studied (i.e., C1-C4), indicating to the theoretically most probably solution. These coefficients are as follows: 1.000 (axis a_0); 0.518 (axis b_0); 0.966 (axis c_0); 0.989 (angle β_0); and 0.997 (volume V_0).

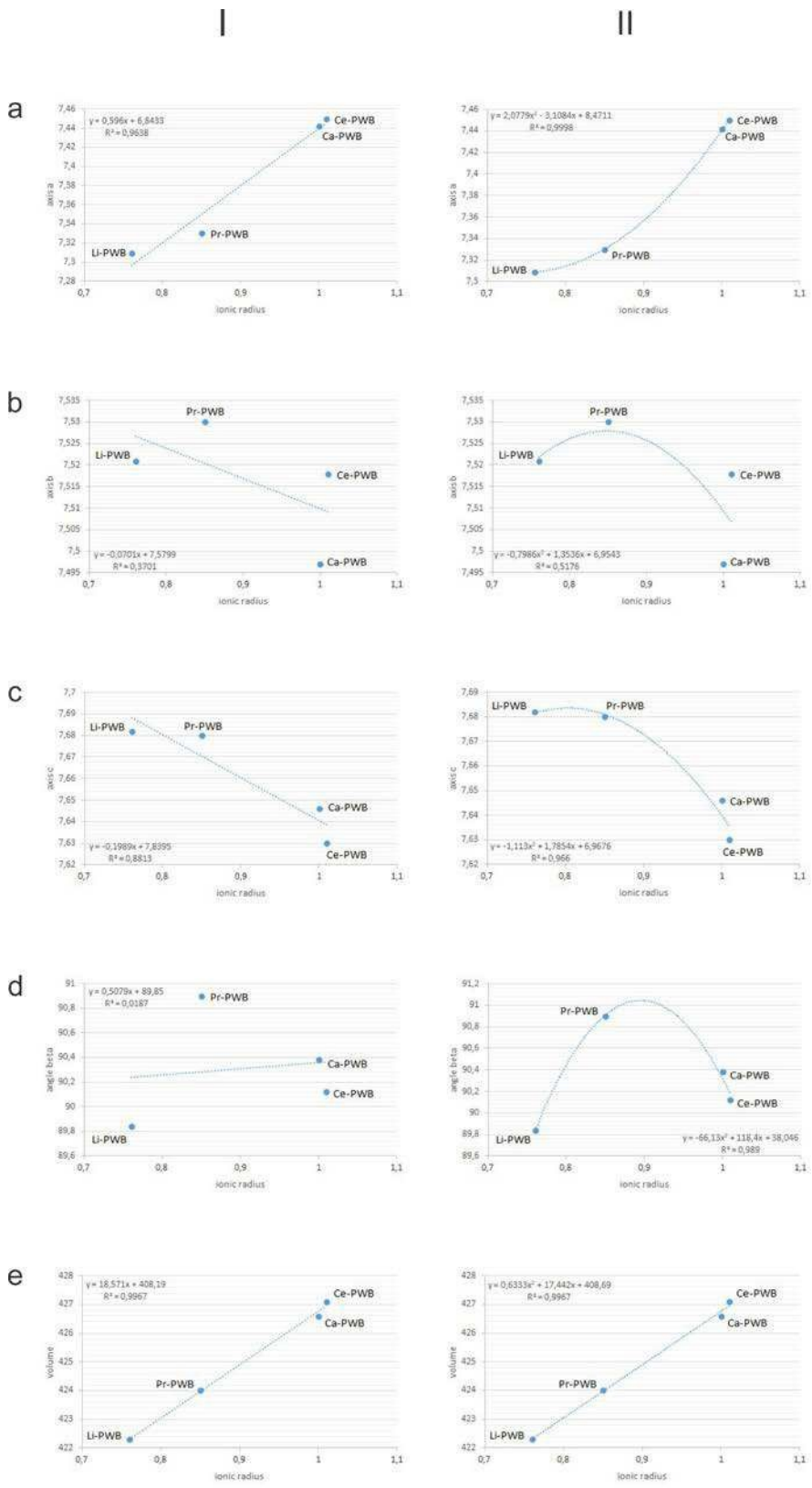

Figure S5 Linear (column I, left) and polynomial (column II, right; C4) variations of ionic radiuses (in Å) for Ce-PWB, Pr-PWB, Ca-PWB and Li-PWB bronzes by: a) axis a_0 (in Å); b) axis b_0 (in Å); c) axis c_0 (in Å); d) angle β_0 (in ^{o}); and e) volume V_0 (in $Å^3$)

Finally, although crystal structure refinements were beyond the scope of this paper, different calculated unit cell dimensions between PWB, Ce-PWB, Pr-PWB, Ca-PWB, and Li-PWB (Table 1), and their more or less different increase-decrease behavior (Figures S2-S5), as well, could be sufficient proof of the various tilting of their WO_6 octahedrons and PO_4 tetrahedrons. Such tilting is caused by different inserted cations into the PWB structure, leading to their different polyhedral distortions, site occupancy factors, bond lengths, angles, etc., which were also confirmed in our studies of some other materials [55,57,58].

Photoluminescent (PL) properties

The PWA, PWB, Ce-PWA, Ce-PWB, Pr-PWA, and Pr-PWB have shown fluorescent properties without characteristic emission peaks of Ce^{3+} and Pr^{3+} (Fig. 8, Fig. S7).

The results of lifetime measurements of pure matrixes and doped samples are presented in Table S4 and Fig. S6.
The CIE chromaticity diagrams have shown that all samples emit in deep blue region which can exhibit potential use as blue emitting source for white light LED's (presented in Fig. 10 and Fig. S7 and coordinates are given in Table S5).

Table S4 The results of lifetime measurements of pure matrixes and doped samples

Sample	**τ_1 (μs)**	**R^2**
PWA	2.91	0.9938
Ce-PWA exc. 320 nm	2.20	0.9845
Ce-PWA exc. 376 nm	1.69	0.9862
Pr-PWA	3.29	0.9834
PWB	2.66	0.9860
Ce-PWB	2.01	0.9850
Pr-PWB	2.70	0.9842

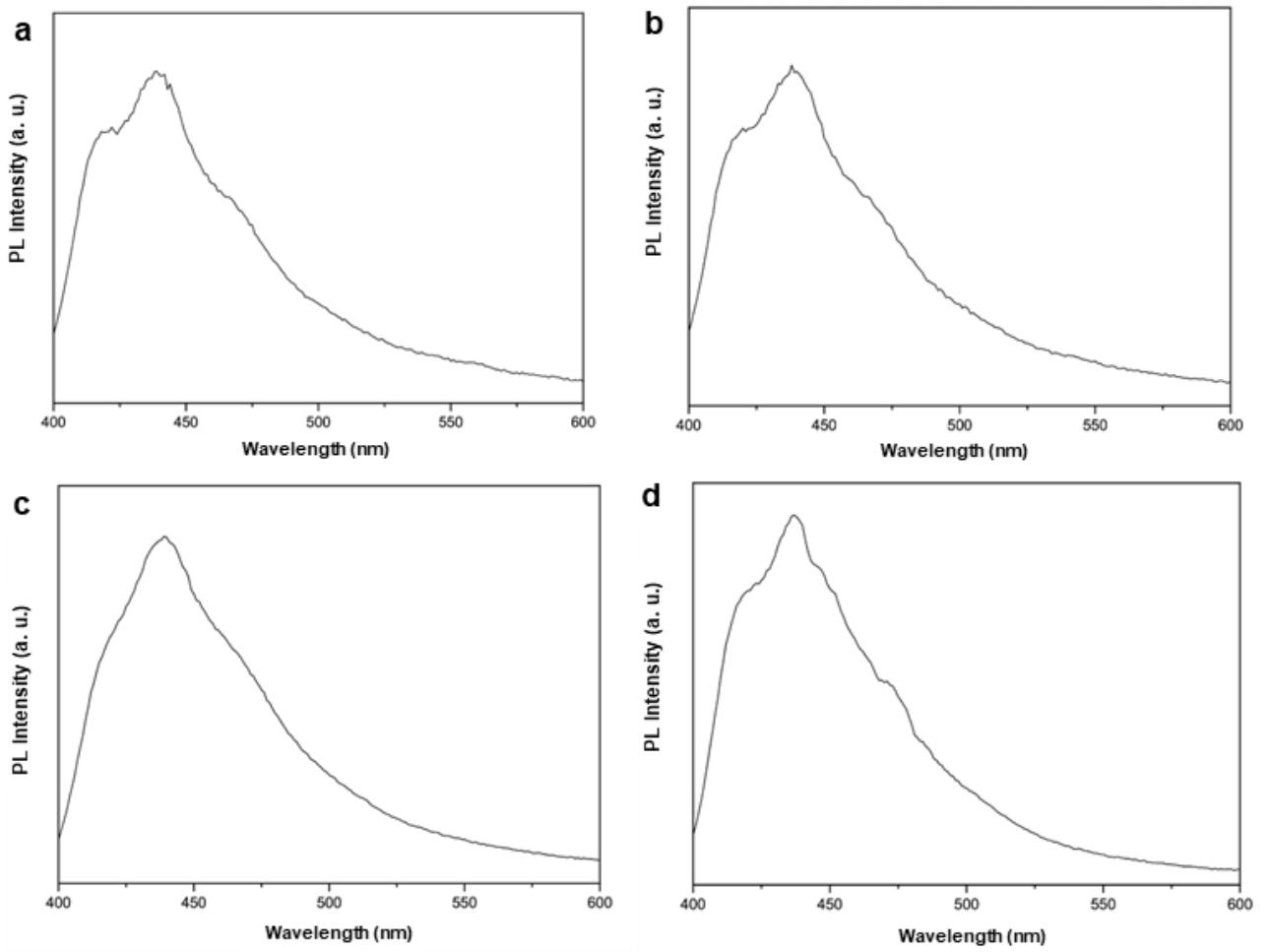

Fig. S6 Emission spectra of: **a** PWA and **b** Ce-PWA excited at 320 nm; **c** Ce-PWA and **d** Pr-PWA under exctiation at 376 nm at room temperature

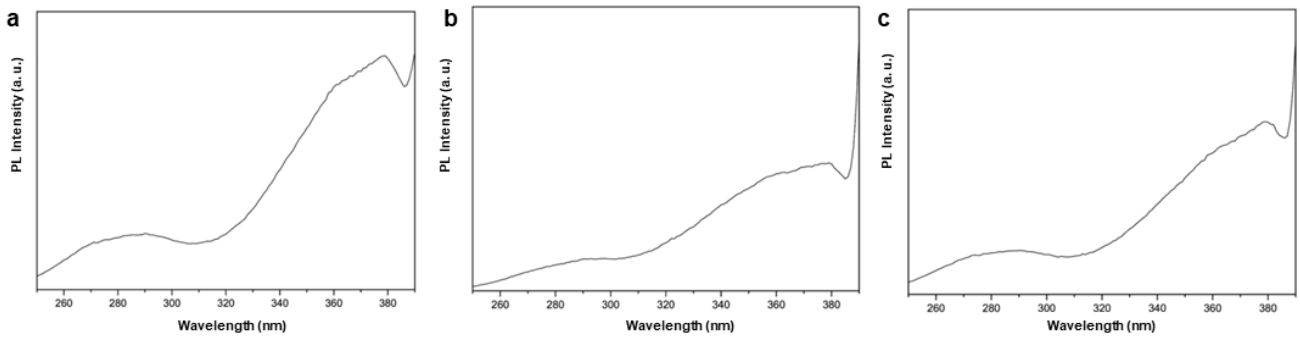

Fig. S7 Excitation spectra of: **a** PWA; **b** Ce-PWA; **c** Pr-PWA emission observed at peak maxima ~ 430 nm at room temperature

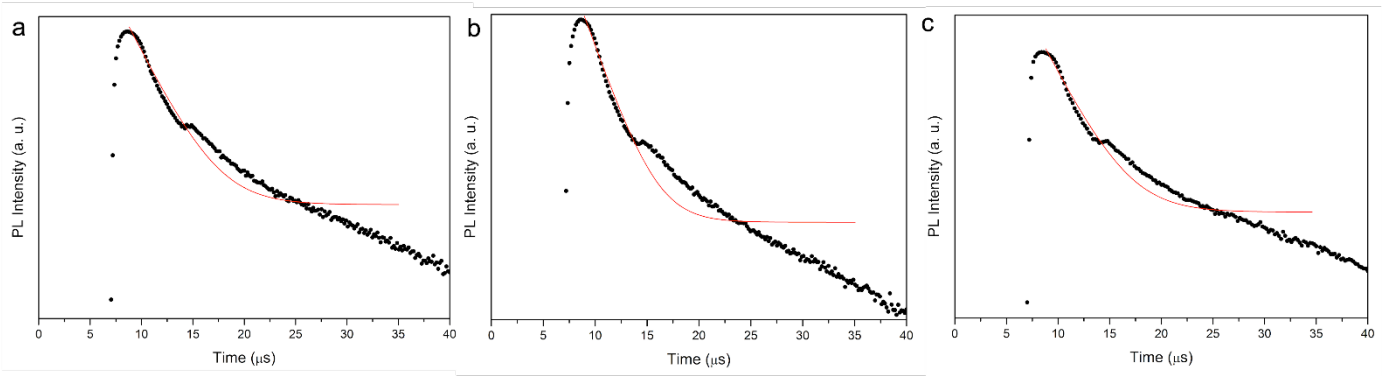

Fig. S8 Decay profiles of: **a** PWB; **b** Ce-PWB; **c** Pr-PWB excited at 376 nm and measured at room temperature

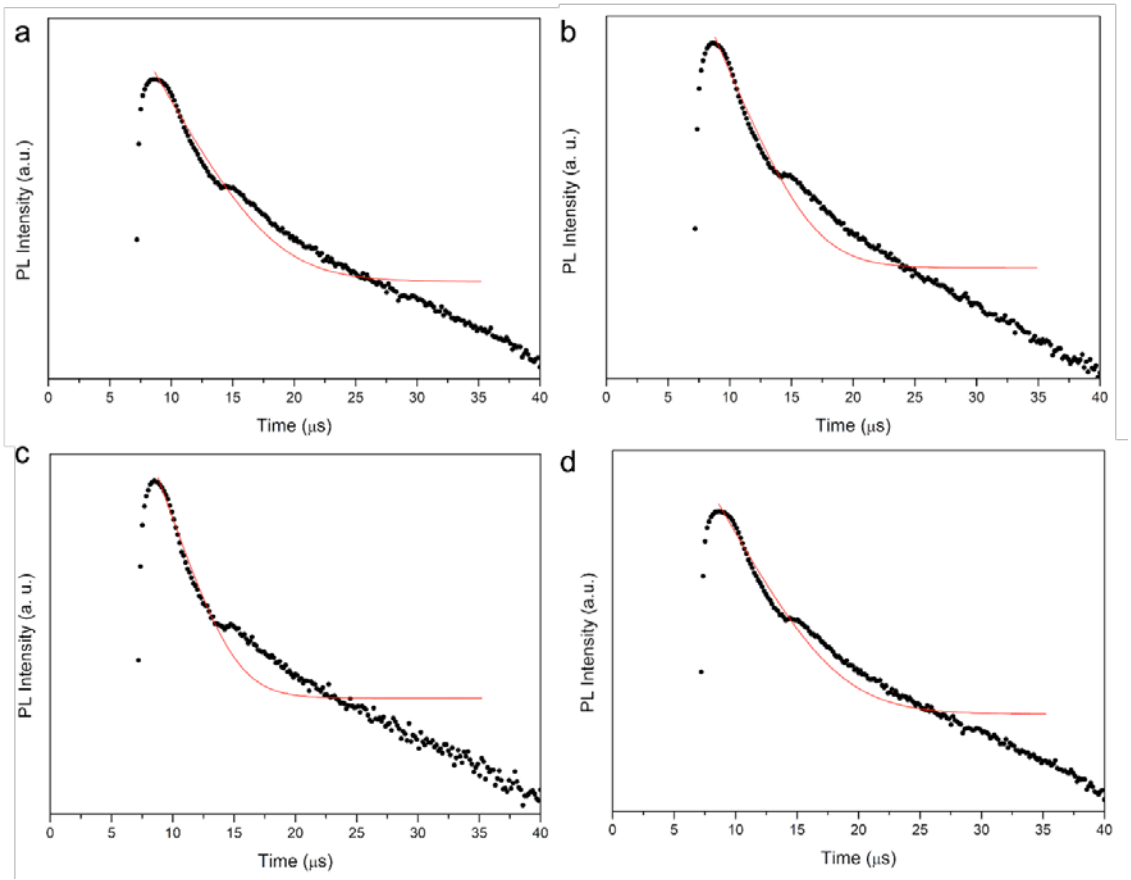

Fig. S9 Decay profiles of: **a** PWA and **b** Ce-PWA excited at 320 nm; **c** Ce-PWA and **d** Pr-PWA excited at 376 nm, measured at room temperature

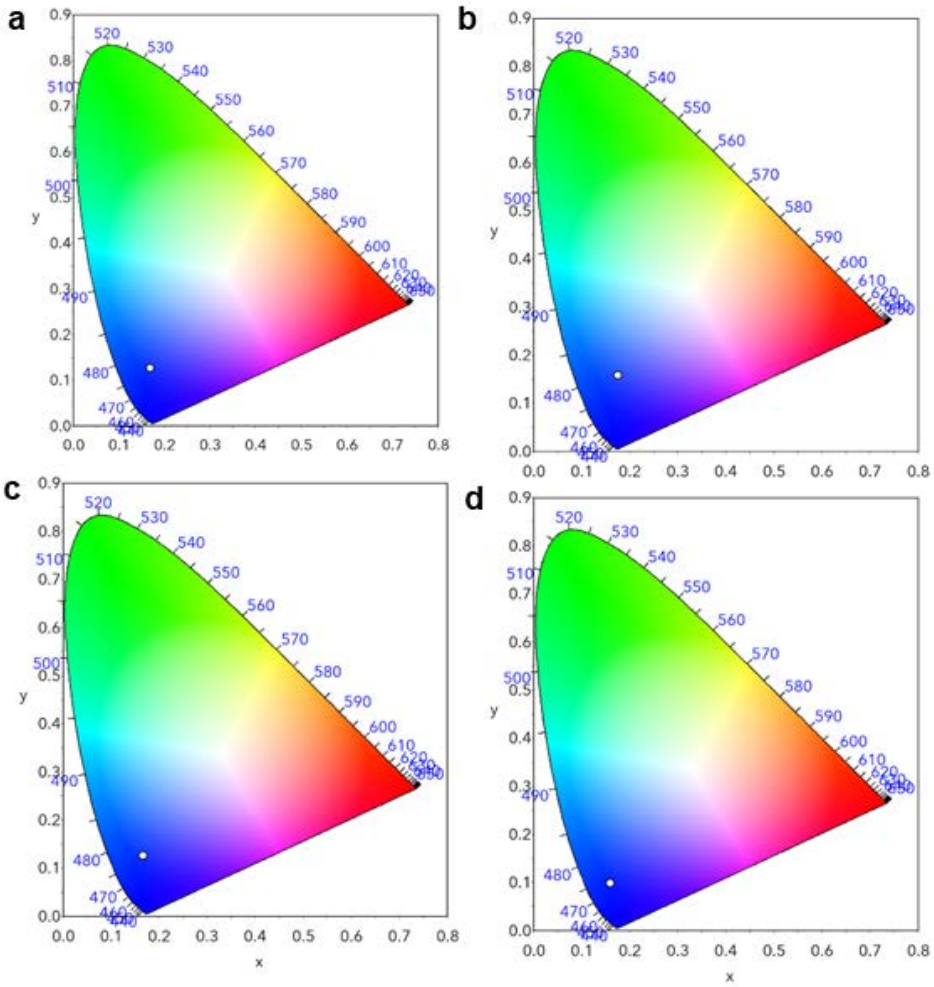

Fig. S10 The CIE chromaticity diagram of: **a** PWA (x = 0.167, y = 0.127) and **b** Ce-PWA (x= 1.175, y = 0.158) excited at 320 nm; **c** Ce-PWA(x = 0.165, y = 0.125) and **d** Pr-PWA (x = 0.158, y = 0.099) excited at 376 nm.